Reaction of Nitric Oxide with Heme Proteins: Studies on Metmyoglobin, Opossum Methemoglobin, and Microperoxidase†

Vijay S. Sharma,* Roger A. Isaacson, Maliyakal E. John, Michael R. Waterman, and Mordechai Chevion

ABSTRACT: Kinetic and EPR studies show that the first step in the reaction of NO with ferric myoglobin, opossum hemoglobin, and microperoxidase is the reversible formation of the H–NO complex: H + NO ⇌ H–NO (where H = Mb^+, or Hb^+ OP, or MP^+). The NO-combination rates are markedly affected by the presence or absence of the distal histidine. The distal histidine significantly reduces the NO-combination rates, perhaps by interaction between the distal histidine and the ferric iron. Thus the β-chains of Hb^+ OP and metmyoglobin show similar combination rates. In the absence of a distal histidine, the NO-combination rates in the α-chains of Hb^+ OP are much faster and similar to those observed for the five-coordinate heme in microperoxidase. The loss of a water molecule from the six-coordination site is assumed to be the rate-limiting step.

In the hemoglobin of the opossum (Hb OP)[1] the α-chains have different residues at positions E7 and E11 than do most other mammalian hemoglobins (Stenzel et al., 1979). The usual histidine at E7 is replaced by Gln and the valine at E11 by Ile. It is an interesting hemoglobin and provides a unique opportunity to study the effect of the distal E7 histidine and the E11 valine on the properties of hemoglobins. The ligand (O_2 and CO) binding properties of ferrous Hb OP reported previously have been explained on the basis of a high allosteric constant L ($L = [Hb^T]/[Hb^R]$; log $L = 6.6$ for Hb OP as compared to 4.5 for Hb A) (Sharma et al., 1982). The ligand combination and dissociation rates in the R and T states of Hb OP differ not more than by a factor of 2 from the rates of the corresponding reactions in Hb A (Sharma et al., 1982). This observation in itself is interesting as high ligand combination and dissociation rates have been reported for Hb Zurich, Hb *Chironomus thummi thummi*, and Hb *Glycera*, which also lack distal histidine (Sharma et al., 1982). Here, we report the results of our kinetic and EPR studies on the reactions of NO with ferric opossum hemoglobin and ferric myoglobin in order to study the role of distal histidine on the reactions of hemoglobins. Of the three gaseous ligands CO, O_2, and NO commonly used in the study of the structure–function relationships in hemoglobins, nitric oxide has the unique distinction of being able to bind to both ferrous and ferric hemoglobins. Keilin & Hartree (1937) have reported that ferric Hb A forms with nitric oxide an easily reversible NO–Hb^+ complex. This compound is unstable and soon after its formation changes to a compound which is indistinguishable from NO–ferrous Hb A. On the other hand, the compound formed by the reaction of Mb^+ with NO, Mb^+–NO, is quite stable (Keilin & Hartree, 1937).

As reported herein, both kinetic and EPR studies provide evidence for the formation of an easily reversible ferric heme–NO complex. The kinetic data indicate that unlike in ferro hemoglobin, in the ferric derivative the distal histidine markedly affects the ligand combination and dissociation rates. The reaction of ferric microperoxidase (MP^+) with NO was used as a model reaction. The NO-combination rates of α-chains in Hb^+ OP and MP^+ are similar. These results suggest that in the absence of the distal histidine, the remaining protein moiety has no effect on NO-combination rates. The most likely rate-limiting step in these reactions is the dissociation of the water molecule from the distal side of the ferric heme.

Materials and Methods

Hemoglobin solutions were prepared by lysing washed red cells with cold water. The opossum blood was obtained from the North American opossum, *Didelphis marsupialis*. Hemoglobin concentrations were calculated by converting Hb OP to the carboxy derivative and using the extinction coefficients for CO–Hb A. Waterman & Stenzel (1974) have reported that the visible spectra of the ferrous derivatives of Hb OP and Hb A are identical.

Standard NO solutions and stripped Hb solutions were prepared as described previously (Waterman & Stenzel, 1974). Sodium salts of IHP, microperoxidase (MP-11), and horse heart myoglobin (type III) were obtained from Sigma Chemical Co. The buffers used were the following: (1) pH 9.2, 0.05 M sodium glycinate in 0.1 M NaCl; (2) pH 7.0 and 6.0, 0.1 M Bis-Tris for stripped hemoglobin solutions or 0.1 M potassium phosphate for hemolysates.

All kinetic experiments were carried out at 20 °C. The combination rates of NO with Hb^+ OP and dissociation from Hb^+ OP–NO were studied by using a Durrum stopped-flow spectrophotometer (Dionex Corp., Palo Alto, CA). Kinetic runs were made at 419 nm at low hemoglobin concentrations (3 μM or less after mixing) or at 565 nm at high hemoglobin concentrations (30 μM or more). The slow reduction rates of NO–Hb^+-OP were obtained on a Beckman DU spectrophotometer equipped with a thermostated cell holder and a strip chart recorder. The faster reduction rates were studied on the stopped-flow spectrophotometer. The solutions of ferric microperoxidase were prepared as described previously (Sharma et al., 1982). Its reaction with NO was studied at 420 nm.

† From the Departments of Medicine and Physics, University of California, San Diego, La Jolla, California 92093 (V.S.S. and R.A.I.), the Department of Biochemistry, The University of Texas, Health Science Center at Dallas, Dallas, Texas 75235 (M.E.J. and M.R.W.), and the Department of Cellular Biochemistry, Hebrew University, Medical School, Jerusalem 91010, Israel (M.C.). *Received January 21, 1983.* This work was supported by Grants AM18781 and AM17348 from the National Institutes of Health, Grant I-624 from the Robert A. Welch Foundation, and Grant DMR 80-07969 from the National Science Foundation.

[1] Abbreviations: Hb OP, opossum hemoglobin; MP, microperoxidase; IHP, inositol hexaphosphate; CTAB, cetyltrimethylammonium bromide; Bis-Tris, 2-[bis(2-hydroxyethyl)amino]-2-(hydroxymethyl)-1,3-propanediol.

0006-2960/83/0422-3897$01.50/0

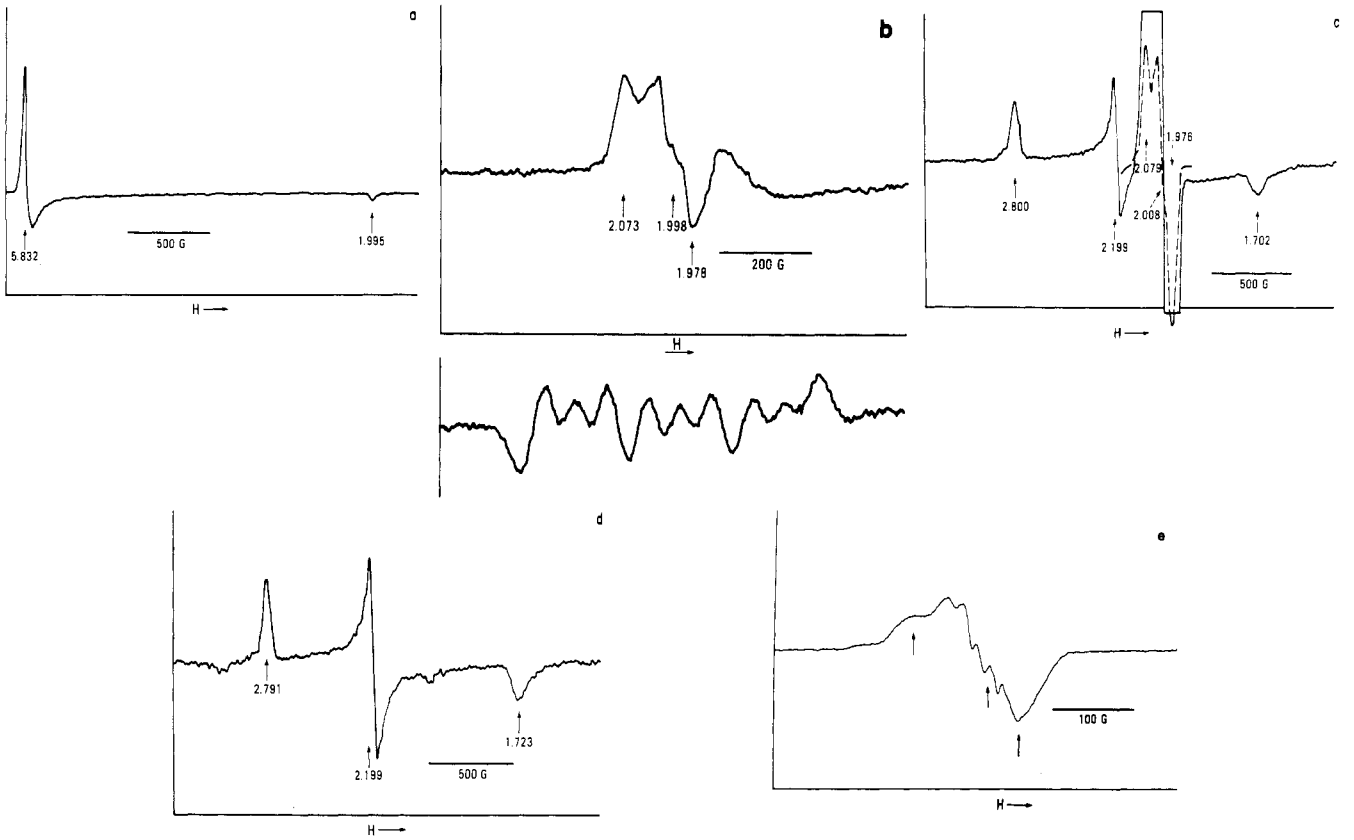

FIGURE 1: Low-temperature first-derivative EPR spectra of opossum hemoglobin at pH 7.0 recorded at 4.1 K. (a) Axial spectrum of aquomet-Hb OP. (b) Upper: Sample b was prepared from sample a by exposing it to NO for 10 min, removing excess NO, and freezing. This spectrum is of ferrous nitrosyl Hb OP. No additional EPR features could be detected in other regions of the magnetic field. Double integration yields 55% of the hemes as ferrous nitrosyl Hb OP, as compared to the total number of hemes in the sample. Lower: Third harmonic spectrum of b in the region of g_{mid}. (c) This sample was prepared by thawing sample b and adding excess N_3^-, anaerobically. Two paramagnetic species are present: the low-spin species azidomet (solid line, g values marked by solid arrows) and the ferrous nitrosyl Hb OP (broken lines) recorded at smaller modulation amplitude (g values marked by broken arrows). (d) Sample a was thawed, and excess N_3^- was added. This spectrum is of low spin azidomet and can be compared to the species that emerged in trace c. (e) Equimolar concentration of IHP was added to met-Hb OP, and the sample was exposed to NO for 10 min and frozen. This spectrum is a ferrous nitrosyl derivative of Hb OP. The three-line superhyperfine structure indicates that the protein resides in a low-affinity form. Double integration yields 52% of the hemes as the ferrous nitrosyl species.

The visible spectra of solutions of Hb^+ OP and Hb^+ OP + NO solutions were recorded on a Cary 14R spectrophotometer. Electron paramagnetic resonance spectra were recorded at 4.1 or 80 K on a superheterodyne spectrometer by using a modulation frequency of 80 s^{-1} and operated by an on-line Nicholet computer (Feher, 1957). Resolution enhancement of the superhyperfine structure of the EPR spectra was obtained by using the third harmonic detection approach (Chevion et al., 1977a,b); typically, a modulation amplitude of 10 G was employed.

Samples were prepared by flushing the methemoglobin opossum solutions (≈0.5 mM) for at least 1 h with ultrapure N_2 followed by 10-min exposure to NO that had been passed through two traps of NaOH. Excess NO was removed by 5-min flushing with N_2, followed by quickly freezing 1.3 mL of solution in Rexolite EPR tubes.

Results

EPR Studies. Figure 1 shows the low-temperature EPR spectra of hemoglobin opossum. At pH 7.0 met-Hb is characterized by an axial spectrum typical for a high-spin aquo derivative (g = 5.832, 5.832, and 1.995; Figure 1a). When this original sample (Figure 1a) was deoxygenated and exposed to NO for 10 min, spectrum 1b (upper) was obtained. This spectrum is reminiscent of nitrosyl derivatives of ferrous hemoglobin A (g = 2.073, 1.998, and 1.978) (Chevion et al., 1977b). The features attributed to ferric iron completely disappeared. Quantitation by double integration and comparison to ferrous Hb OP–NO showed that ≈55% of the expected number of spins could be accounted for. No apparent superhyperfine structure was noticed at the g_z region of the first derivative spectrum. Using the third harmonic detection approach (Chevion et al., 1977a) led to the appearance of a nine-line superhyperfine pattern centered at g = 2.0045 that could be analyzed as a triplet of triplets. The main triplet shows a 22.6 ± 0.5 G splitting while each of the small tripleta arise from additional interaction characterized by a splitting of 7.5 ± 0.3 G (1b lower).

When the sample 1b was thawed and excess azide added anaerobically, the sample was refrozen and its EPR spectrum recorded (Figure 1c), two paramagnetic species were apparent. One was the same nitrosyl derivative of ferrous Hb OP (g = 2.079, 2.008, and 1.976), while the second species was the low-spin metazide derivative of Hb OP (g = 2.800, 2.199, and 1.702). For comparison, excess azide was added to the original sample of met-Hb OP (Figure 1a), and the new spectrum was recorded (Figure 1d) (g = 2.791, 2.199, and 1.723).

The effect of IHP on the reaction between nitric oxide and methemoglobin opossum was investigated. When IHP was added to the high-spin aquomet species at pH 7.0 (sample 1a), the same axial structure was maintained (g = 5.838, 5.838, and 1.996; not shown). Subsequent exposure of the IHP-containing solution to NO for 10 min led to the formation of the nitrosyl spectrum 1e (g = 2.063, 2.012, and 1.984). Unlike spectrum 1b spectrum 1e consists of a three-line superhyperfine structure at g_z with a splitting of 16.7 ± 5 G. In addition, the

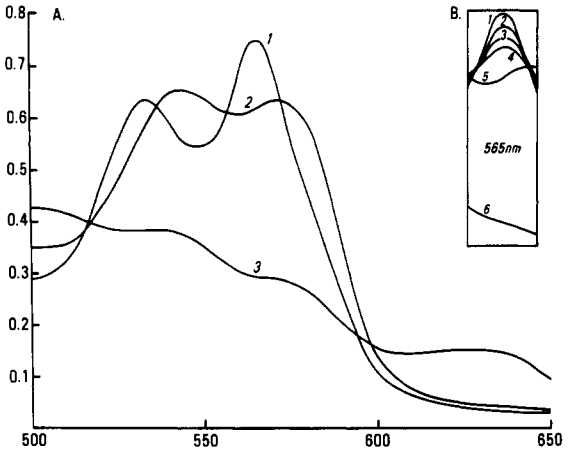

FIGURE 2: Visible spectra of Hb^+ OP plus NO solutions. [Hb^+OP] = 50 μM; [NO] = 1911 μM; 0.1 M Bis-Tris, pH 7.0, T = 20 °C. (A) (Curve 1) Within 10 min of adding NO; (curve 2) after 20 h; (curve 3) ferric Hb OP without NO. (B) (Curve 1) After 30 min of adding NO; (curves 2–4) at 1-h intervals; (curve 5) next day, approximately after 20 h; (curve 6) ferric Hb OP, without NO.

double integral for this sample accounted for 52 ± 6% of the expected spins when compared to the ferrous derivative of hemoglobin opossum. Consequent addition of N_3^- to the sample gave rise to the low-spin metazide derivative.

In a series of EPR experiments conducted at pH 9.34, results similar to those shown in Figure 1b,c were obtained. Under these conditions, the methemoglobin resides in the R state and is predominantly low-spin hydroxymet (g = 2.491, 2.167, and 1.880). The exposure of this sample to NO for 10 min gave rise to the nitrosyl derivative spectrum (g = 2.071, 2.004, and 1.973) in which half of the spins were accounted for, but no hyperfine structure was apparent. Using the third harmonic detection approach yielded the nine-line spectrum centered at 2.0044 that could be analyzed as a triplet of triplets with splittings of 22.2 ± 0.3 and 6.9 ± 0.5 G. Likewise, the addition of N_3^- to this sample led to the restoration of additonal features ascribed to the low-spin met azide spectrum.

Visible Spectrum. Figure 2 shows the visible spectra of Hb^+ OP and its nitrosyl derivatives. Curve A1 was obtained soon after NO was added to Hb^+ OP: λ_{max} at 534 and 565 nm. These should be compared with λ_{max} reported for Mb^+–NO: 530 and 572 nm (Wittenberg et al., 1967). The spectrum of Hb^+ OP–NO changes with time as shown in curves 1–5 in Figure 2B. The rate of absorbance change depends inversely on NO concentration and will be discussed under Kinetic Studies. Curves A2 and B5 were recorded after about 20 h of adding NO to Hb^+ OP solution. There was no further change in the spectrum. The curves remained unchanged on addition of dithionite and more NO and were indistinguishable from the spectrum of ferrous Hb OP–NO. The maxima are at 545 and 575 nm. Curves A3 and B6 are for Hb^+ OP without NO.

Kinetic Studies. (A) Reaction of Mb^+ with NO. The pseudo-first-order rate constants (k_{obsd}) for the reaction of Mb^+ with NO are plotted as a function of [NO] in Figure 3. The intercept and the slope yield the dissociation and combination rate constants, respectively, for the reaction

$$Mb^+ + NO \underset{k'}{\overset{k}{\rightleftharpoons}} Mb^+\text{–}NO$$

$$k_{obsd} = k([NO] + [Mb^+]) + k' = k[NO]_{tot} + k'$$

when $[NO]_{tot} \gg [Mb^+]_{tot}$ (Antonini & Brunori, 1971); tot = total stoichiometric concentration, and k_{obsd} = the observed

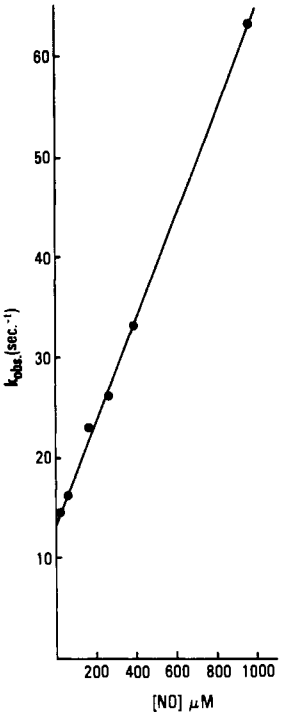

FIGURE 3: Observed rates plotted against [NO] for the reaction of NO with ferric myoglobin. λ = 419 nm; [Mb^+] = 1.5 μM, 0.1 M Bis-Tris, pH 7.0.

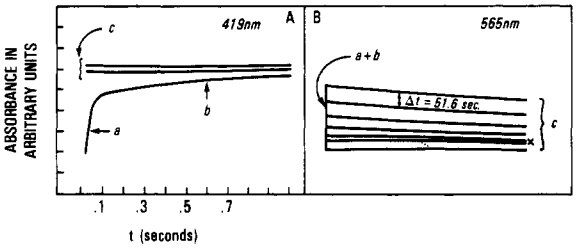

FIGURE 4: Reaction time course for the reaction of [NO] with Hb^+ OP. (A) λ = 419 nm; [Hb^+OP] = 2.7 μM; [NO] = 27.8 μM; a = the fast phase; b = the slow phase; c = the very slow phase. (B) The very slow phase shown in greater detail. λ = 565 nm; [Hb^+OP] = 20 μM; [NO] = 12.5 μM. 0.1 M Bis-Tris, pH 7.0, for both (A) and (B). After the trace x the absorbance changes were small, and successive traces were not separated. The last trace, however, gives the value of A_∞ accurately.

pseudo-first-order rate constant, obtained from the slopes of ln ($A_\infty - A_t$) vs. time plots at several NO concentrations; k = 5.3 × 10^4 M^{-1} s^{-1} and k' = 14 s^{-1}.

The positive intercept indicates the reversible nature of the reaction. The spectrum of Mb^+–NO has been reported by Wittenberg et al. (1967).

(B) Reaction of Hb^+ OP with NO. Figure 4 shows a typical reaction time course for the reaction of NO with Hb^+ OP. Three distinct phases are clearly observed. These will be referred to as the fast phase (f), slow phase (s), and very slow phase (vs). The reaction rates for each phase were obtained at two hemoglobin concentrations (2 and 50 μM) as a function of NO concentration.

Fast Phase. In Figure 5 the pseudo-first-order rate constants (k_{obsd}) are plotted as a function of NO concentration. The intercept and the slope yield the values of the "off" and "on" rate constants, respectively:

$$Hb^+ OP + NO \underset{k'}{\overset{k}{\rightleftharpoons}} Hb^+ OP\text{–}NO$$

$$k_{obsd} = k[NO]_{tot} + k'$$

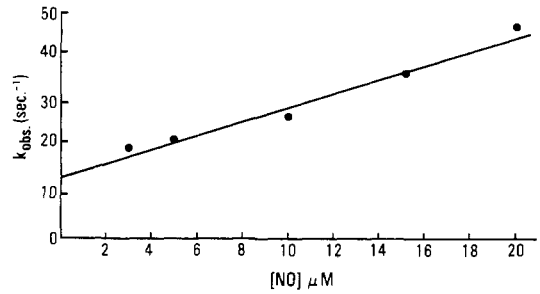

FIGURE 5: Observed rates plotted against [NO] for the fast phase of Hb^+ OP; λ = 419 nm. [Hb^+ OP] = 0.5 μM; 0.1 M Bis-Tris, pH 7.0.

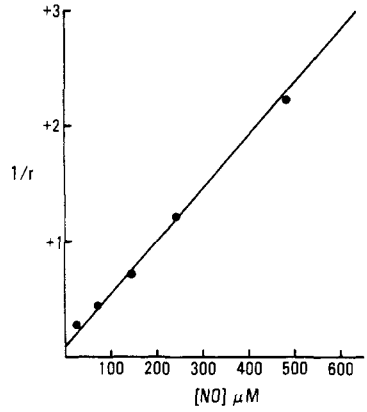

FIGURE 6: Reaction of Hb^+ OP with azide under varying concentrations of nitric oxide. λ = 565 nm. [N_3^-] = 0.01 M; [Hb^+ OP] = 25 μM; 0.1 M Bis-Tris, pH 7.0.

when $[NO]_{tot} \gg [Hb^+ OP]_{tot}$; $k = 1.3 \times 10^6$ M^{-1} s^{-1} and $k' = 13$ s^{-1}.

The positive intercept in Figure 5 indicates the reversible nature of the reaction. This point was further investigated by the method of Gibson & Roughton (1955). Hb^+ OP was reacted with azide, in the presence of varying concentrations of nitric oxide. Figure 6 gives a plot of $1/r$ vs. [NO]. r, the observed first-order rate constant in the present case, represents the average of the NO-dissociation rate constants of the slow and fast components (see below). The intercept in this case gives $1/r = 0.12$, yielding a value of 8.33 s^{-1} for r. This is in good agreement with the value expected on the basis of data in Figures 5 and 7 (8 s^{-1}).

Later on it will be pointed out that the very slow phase represents the reduction of the species Hb^+ OP–NO to the ferrous derivative. In order to avoid significant depletion of Hb^+ OP–NO due to the vs reaction, the reaction of Hb^+ OP with azide in the presence of varying concentrations of NO was studied in double mixing experiments. In these experiments first NO is mixed with Hb^+ OP in the stopped-flow instrument. The mixture is aged (in the first mixing chamber) long enough to complete the NO-combination reaction and then reacted with azide in the second mixing.

Slow Phase. At high NO concentrations most of the reaction corresponding to the fast phase is complete within the mixing time of the stopped-flow instrument. The very slow phase becomes extremely slow (for reasons to be discussed in the next section). The slow phase, therefore, can be studied without difficulty under these conditions. A plot of pseudo-first-order rates vs. [NO] gave a straight line with intercept = 2.9 (Figure 7). The slope yielded the combination rate constant equal to 1.68×10^4 M^{-1} s^{-1}.

Very Slow Phase. After the completion of reactions corresponding to fast and slow phases, a very slow reaction is

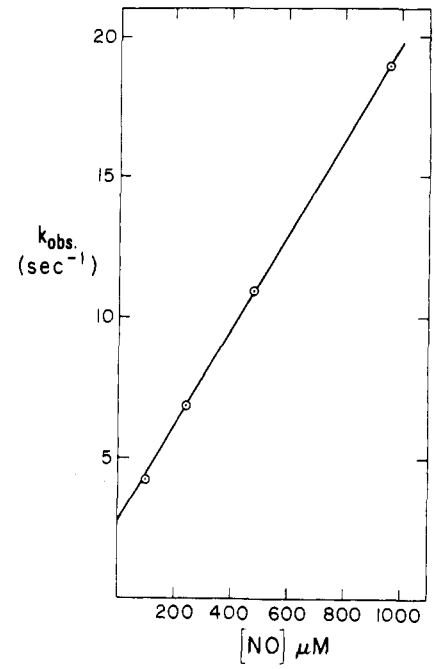

FIGURE 7: Observed rates plotted against [NO] for the slow phase of Hb^+ OP. λ = 565 nm; [Hb^+ OP] = 35 μM; 0.1 M Bis-Tris, pH 7.0. The data point at 96 μM [NO] was obtained at 2 μM [Hb^+ OP].

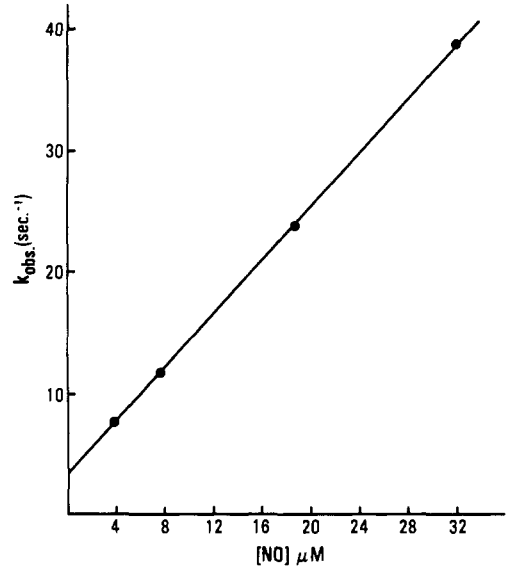

FIGURE 8: Observed rates plotted against [NO] for the reaction of NO with ferric microperoxidase. λ = 420 nm; 0.1 M Bis-Tris, pH 7.0; [MP^+] = 0.5 μM after mixing.

observed. The direction of the absorbance change for this reaction corresponds to absorbance changes observed when curve A1 changes to curve A2 in Figure 2. At NO concentrations less than [Hb^+ OP], the reaction rates vary inversely with NO concentrations. At high NO concentrations (400–1900 μM) the reaction rates become very slow and independent of NO concentration. The first-order rate constant under these conditions is 4×10^{-5} s^{-1}. In the region of dependence on NO concentration, the reaction rates show considerable scatter in different preparations of met-Hb OP, and as [NO] → 0, the observed rate constants varied in the range 0.007–0.03 s^{-1} (in four Hb^+ OP preparations).

(C) Reaction of NO with Microperoxidase (MP^+). The reaction of MP^+ with NO was predominantly monophasic. In Figure 8 the reaction rates are plotted against NO concentration. From the slope and the intercept, the following rate

Table I: Rate Constants for the Reaction of NO with Mb^+, Hb^+ OP, and MP^+

sample	on [k (M^{-1} s^{-1})]	off [k' (s^{-1})]
Mb^+	5.3×10^4	14
Hb^+ OP α-chains	1.3×10^6	13
Hb^+ OP β-chains	1.68×10^4	2.9
MP^+	1.1×10^6	3.4

[a] $T = 20$ °C. Buffer = 0.1 M Bis-Tris, pH 7.0.

constants are obtained: $k = 1.1 \times 10^6$ M^{-1} s^{-1} and $k' = 3.4$ s^{-1}. These rates are assigned to the reaction

$$MP^+ + NO \underset{k'}{\overset{k}{\rightleftharpoons}} MP^+\text{–}NO$$

The kinetic data are listed in Table I.

Discussion

Both kinetic and EPR studies indicate that the first step in the reaction of NO with opossum methemoglobin is the formation of the reversible species Hb^+ OP–NO. Exposure of met-Hb OP to NO led to the appearance of an EPR spectrum characteristic of nitrosyl derivatives of ferrous hemoglobins (Figure 1a,b) (Chevion et al., 1977b). The quantitation of this species indicates that the reduction of only half of the hemes took place in the time range of EPR experiments, while the other half of the protein was EPR silent, because of the formation of the complex Hb^+ OP–NO, in which two paramagnetic species, the low-spin ferric heme and the NO, are in close proximity. Such structure gives rise to antiparamagnetic spin-coupling interaction rendering both species EPR silent. However, unlike the strong binding of NO to ferrous hemoglobin, in the case of met-Hb OP the NO is easily exchangeable and could easily be replaced by azide or cyanide. An analogous complex has been suggested for met-Mb–NO (Wittenberg et al., 1967) and has been confirmed by us.

The valence hybrids produced in the reaction between NO and Hb^+ OP contain hemes which are 50% reduced and bound to NO. This may indicate that only one type of subunits, either the α- or the β-chains, has been reduced. As the β-chains have the distal histidine conserved, these chains are expected to react similarly to myoglobin or human β-chains. When Hb^+ A or Mb^+ reacts with NO, a stable ferric–NO complex is formed, and the rate of its reduction to ferrous–NO is extremely slow (Wittenberg et al., 1967; Keilin & Hartree, 1937). Thus, this may suggest that in Hb^+ OP the α-chains have been reduced. A substantiation to this idea is provided from the superhyperfine structure of the EPR spectrum of the hybrid. While NO–β chains always show a nine-line pattern (Chevion et al., 1977b; John & Waterman, 1979a,b), the EPR spectrum of NO–α subunits switch between the three-line and nine-line patterns upon the transition in the quaternary structure of the tetramer (T → R) (Chevion et al., 1977a,b; John & Waterman, 1979a,b). Here, at pH 7.0 and in the presence of IHP, a clear three-line pattern is observed, while in the absence of organic phosphates a nine-line pattern can be identified. In summary, it is suggested that the structure of the valence hybrid is $\alpha_2^{NO}\beta_2^{+NO}$.

Identification of the Three Phases Observed in the Kinetic Experiments with Three Chemical Reactions. (a) The *very slow phase* can be unambiguously assigned to the reduction of ferric Hb^+ OP–NO complex to the ferrous Hb OP–NO complex. In nitrosyl derivatives of Mb^+, Hb^+ A, and ferric peroxidase (Wittenberg et al., 1967) the wavelength of maximum absorption (λ_{max}) moves from 533 and 566 nm in ferric derivatives to 545 and 575 nm in ferrous derivatives. The visible spectra of ferric and ferrous nitrosyl derivatives of Hb OP are consistent in this regard. The rates of reduction vary inversely with NO concentration, suggesting that unliganded and/or partially liganded species are involved in the rate-limiting reaction. This is reminiscent of the autooxidation reaction of Hb A which proceeds more rapidly when the material is partly deoxygenated (George & Stratmann, 1952). (b) The remaining two phases (i.e., the *fast and slow*) are observed even at pH 9.2 and a very low heme concentration of 2.5 μM. The relative proportion of the two phases remains the same at pH 7 and pH 9.2:

$$\frac{\Delta[A](\text{due to fast phase})}{\Delta[A]_{tot}} = 0.29$$

These observations rule out the possibility of two different conformations or structures of ferric Hb OP being responsible for the fast and slow phases of the reaction. It appears that these two phases (f and s) represent the reactions of ferric α- and β-chains with NO.

The residues in the heme pocket of myoglobin and β-chains of opossum hemoglobin are similar, and therefore, the similarity of the NO-combination rate constants of the slow phase and myoglobin suggests that the slow phase in the reaction of NO with Hb^+ OP most likely represents the reaction with the β-chains. The assignment of the slow phase to the reaction of β-chains is also supported by our preliminary data on the NO combination and dissociation rate constants of methemoglobin A ($k_{on} = 5 \times 10^3$ M^{-1} s^{-1}; $k_{off} = 4$ s^{-1}).

There is a large difference in the NO combination rate constants of α^+- and β^+-chains of Hb^+ OP, and these rates particularly of β^+-chains are much slower than the rates for the combination of NO with ferrous hemoglobins ($>10^7$ M^{-1} s^{-1}) (Cassoly & Gibson, 1976). In our studies on the reactions of ferrous Hb OP we observed that the ligand combination and dissociation rate constants of α- and β-chains were the same and did not differ much from those of Hb A (Sharma et al., 1982). These rates were not nearly as high as those reported for Hb Zurich, Hb *Chironomus thummi thummi*, and Hb *Glycera*, all of which have substitutions at the distal histidine residue (Sharma et al., 1982 and references therein). From these observations we concluded that the unusually high CO-combination rate constants in the hemoglobins mentioned above may not be due to the substitution of distal histidine per se but may be due to the wide open heme pocket which allows ligand easy access to the heme iron. This explanation, although consistent with the X-ray crystallographic data (Tucker et al., 1978) on Hb Zurich, is open to the criticism that Gln at position E7 in the α-chains of opossum might be sterically similar to histidine in Hb A. The data presented here show clearly that this is not so; Gln at E7 in the α-chains of Hb OP is not sterically similar to His-E7.

In the ferric derivative, the distal histidine significantly slows down the NO-combination rates, as we observe in Mb^+ and β^+ of Hb OP. This observation suggests either direct or indirect (via the water molecule on the distal side in aquomet-Hb) interaction between the distal histidine and the ferric heme. Furthermore, the NO-combination rate constant for the α-chains of Hb^+ OP is similar to that for MP^+; this is consistent with the absence of distal histidine in these two molecules. The rate-limiting step in these reactions is most probably the loss of the water molecule from the six-coordination site of ferric heme. In the presence of the distal histidine, the water molecule at the ligand binding site can be stabilized by hydrogen bonding with the distal histidine side

chain. In the absence of this histidine and water molecule at the ligand binding site, very high ligand (N_3^-) combination rates have been reported for Mb^+ aplysia (Giacometti et al., 1981).

Acknowledgments

We thank Dr. Helen Ranney for helpful discussions.

Registry No. MP-11, 30975-71-4; nitric oxide, 10102-43-9; histidine, 71-00-1.

References

Antonini, E., & Brunori, M. (1971) *Front. Biol. 21*, 194.
Cassoly, R., & Gibson, Q. H. (1976) *J. Mol. Biol. 91*, 301-313.
Chevion, M., Blumberg, W. E., & Peisach, J. (1977a) *Metal-Ligand Interaction in Organic and Biochemistry* (Pullman, B., & Goldblum, N., Eds.) pp 153-162, D. Reidel Publishing Co., Dordrecht, Holland.
Chevion, M., Traum, M. M., Blumberg, W. E., & Peisach, J. (1977b) *Biochim. Biophys. Acta 490*, 272-278.
Feher, G. (1957) *Bell Syst. Tech. J. 26*, 449-484.
George, P., & Stratmann, C. J. (1952) *Biochem. J. 51*, 103.
Giacometti, G. M., Ascenzi, P., Brunori, M., Rigatti, C., Giacometti, G., & Bolognesi, M. (1981) *J. Mol. Biol. 151*, 315-319.
Gibson, Q. H., & Roughton, F. J. W. (1955) *Proc. R. Soc. London, Ser. B 143*, 310-334.
John, M. E., & Waterman, M. R. (1979a) *J. Biol. Chem. 254*, 11953-11957.
John, M. E., & Waterman, M. R. (1979b) *FEBS Lett. 106*, 219-222.
Keilin, D., & Hartree, E. F. (1937) *Nature (London) 139*, 548.
Sharma, V. S., John, M. E., & Waterman, M. R. (1982) *J. Biol. Chem. 257*, 11887-11892.
Stenzel, P., Brimhall, B., Jones, R. T., McLachlin, A., & Gibson, D. (1979) *J. Biol. Chem. 254*, 2071-2076.
Tucker, P. N., Philips, S. E. V., Perutz, M. F., Houtchins, R., & Caughey, W. S. (1978) *Proc. Natl. Acad. Sci. U.S.A. 75*, 1076-1080.
Waterman, M. R., & Stenzel, P. (1974) *Biochim. Biophys. Acta 359*, 401-410.
Wittenberg, J. B., Noble, R. W., Wittenberg, B. A., Antonini, E., Brunori, M., & Wyman, J. (1967) *J. Biol. Chem. 242*, 626-634.

Isolation and Spectral Studies on the Calcium Binding Properties of Bovine Brain S-100a Protein†

Rajam S. Mani and Cyril M. Kay*

ABSTRACT: The brain-specific S-100 protein is a mixture of two predominant isomers, S-100a and S-100b, which exist in brain tissue in almost equal amounts. The subunit compositions of S-100a and S-100b are $\alpha\beta$ and β_2, respectively. S-100a, isolated in the present study by using hydroxylapatite chromatography in its final purification, is homogeneous by the criteria of gel electrophoresis in the absence and presence of sodium dodecyl sulfate. The S-100a protein undergoes a conformational change upon binding calcium, as indicated by ultraviolet (UV) difference spectroscopy, circular dichroism (CD) studies in the aromatic and far-UV spectral regions, and fluorescence measurements. The binding affinity of Ca^{2+} to S-100a was studied at two pH values, 8.3 and 7.5. The effect of Ca^{2+} binding on the UV absorption difference spectrum and fluorescence emission spectrum was different at these two pH values. When the apoprotein at pH 8.3 was excited at 280 nm, the emission maximum was located at 335 nm. In the presence of Ca^{2+}, the emission maximum occurred around 339 nm and was accompanied by a nearly 60% increase in fluorescence intensity. Fluorescence titration of S-100a with Ca^{2+} indicated the presence of two calcium binding sites on the protein at pH 8.3 with K_d values of 5.5×10^{-5} M and 2.5×10^{-4} M, whereas at pH 7.5, the protein possesses only one Ca^{2+} binding site with a K_d of 1.2×10^{-4} M. The effect of K^+ on the protein was antagonistic to that of calcium. Although the affinity of both S-100 proteins for calcium is similar and pH dependent, subtle differences exist in the microenvironment of specific chromophores. Near-UV CD studies revealed that the environments around the tyrosine and phenylalanine residues are different in the two S-100 proteins. UV difference spectroscopy also suggests that the single tryptophan and the tyrosine chromophores in S-100a are blue shifted (i.e., exposed to the solvent) in the presence of Ca^{2+}, in contrast to the observed red shift noted with S-100b.

The S-100 protein is a nervous tissue specific protein widely distributed in the nervous systems of various vertebrates (Moore, 1965, 1972). This protein is found primarily in glial cells (Ludwin et al., 1976) and represents up to 0.2% of the total soluble brain protein. Recently, Gayner et al. (1980) have show the presence of S-100 protein in continuous cell lines of human malignant melanoma. The biological function of this protein is unknown; however, existing literature suggests a role for it in the function or development of the nervous system (Hyden & Lange, 1970; Calissano & Bangham, 1971; Calissano et al., 1974).

S-100 protein is actually a mixture of two predominant isomers, S-100a and S-100b with a subunit composition of $\alpha\beta$ and β_2, respectively (Isobe & Okuyama, 1981). The amino acid sequences of S-100 proteins have been determined (Isobe & Okuyama, 1978, 1981). The S-100b protein polypeptide chain (β-subunit) consists of 91 amino acid residues, and its sequence is similar to calcium binding proteins such as calmodulin (Cheung, 1980; Kasai et al., 1980), troponin C (Van Eerd & Takahashi, 1975), and parvalbumin (Perchere &

† From the Medical Research Council Group in Protein Structure and Function, Department of Biochemistry, University of Alberta, Edmonton, Alberta, Canada T6G 2H7. *Received January 26, 1983.* This investigation was generously supported by the Medical Research Council of Canada and the Alberta Heritage Foundation for Medical Research.

0006-2960/83/0422-3902$01.50/0